A study of the reaction $\tilde{\nu}_e + p \to e^+ + n$ on a nuclear reactor

A. I. Afonin, S. N. Ketov, V. I. Kopeĭkin, L. A. Mikaelyan, M. D. Skorokhvatov, and S. V. Tolokonnikov

I. V. Kurchatov Institute of Atomic Energy, Academy of Sciences of the USSR, Moscow

(Submitted 29 May 1987)
Zh. Eksp. Teor. Fiz. **94**, 1–17 (February 1988)

Inverse neutron beta decay, $\tilde{\nu}_e + p \to e^+ + n$, was studied in a series of experiments performed at the Rovno Nuclear Power Station. Measurements were made of the absolute cross sections for the reaction, and the positron spectrum was recorded at a distance of 18 m from the reactor. A relative comparison was also carried out between the intensities and the spectra at distances of 18 and 25 m. The measured reaction cross section was found to be $^5\sigma_f(6.28 \pm 5\%) \times 10^{-43}$ cm^2/fission, and it was shown that the probabilities of forward and reverse reactions were equal to within experimental uncertainty. The axial beta-decay constant was found to be $g_A = 1.775 \times 10^{-43}$ erg·cm$^3 \pm 3.5\%$. Upper limits were obtained for the Pontecorvo oscillation parameters. The oscillation effects reported for the Bugey reactor in 1984 were not confirmed.

I. INTRODUCTION

1. In their 1953–1956 experiments on a nuclear reactor, Reines *et al.*[1-3] detected free neutrinos using the reaction

$$\tilde{\nu}_e + p \to e^+ + n \qquad (1)$$

and estimated its cross section. Since then, interest in this reaction has increased very considerably. It has been under investigation in the neutrino experiments[4] that have continued since 1982 on the reactor of the Rovno Nuclear Power Station (RNPS), but it has also been the means whereby the properties of the electron antineutrino $\tilde{\nu}_e$ have been investigated. (The use of the symbol $\tilde{\nu}_e$ is intended to show that we are dealing with a particle that is produced together with the electron in β^- decay.)

Reaction (1) and related processes such as nuclear $\beta^\pm$ decay, electron capture, the $p + p + e^- \to d + \nu_e$ reaction in stars, and so on, are described at low energies by the universal V–A interaction between charged currents of leptons and nucleons, characterized by two fundamental constants, namely, the vector (g_V) and the axial (g_A) constants. These constants appear in the cross section for reaction (1) and in the decay of the free neutron in the form of the grouping $g_V^2 + 3g_A^2$:

$$\sigma_0(E_\nu) = \pi^{-1}(g_V^2 + 3g_A^2) p_e E_e, \qquad (2)$$

$$E_e = E_\nu - (M_n - M_p) = E_\nu - 1.293 \text{ MeV}, \qquad (3)$$

where E_ν, p_e, and E_e are, respectively, the energy of the antineutrino $\tilde{\nu}_e$, the positron momentum, and positron energy.[1)]

The increasing precision of neutrino experiments has meant that we can now consider the independent determination of the beta-decay constants and the verification of the equality of the probabilities of forward and inverse reactions. We recall that vector current conservation can be used to determine the constant g_V with high precision by analyzing $0^+ \to 0^+$ beta-transitions in mirror nuclei: $g_V = (1.4127 \pm 0.0003) \times 10^{-49}$ erg·cm^3 (Ref. 5). On the other hand, the axial interaction in its purest form appears only at low energies in free-nucleon reactions such as (1) and the beta decay of the neutron.

The energy dependence of the cross section (2) and the energy equation (3) together lie at the basis of neutrino spectroscopy. Direct measurement of the true $\tilde{\nu}_e$ spectrum is essential for the interpretation of neutrino experiments on reactors and, in particular, for the investigation of the interaction between $\tilde{\nu}_e$ and the deuteron, planned for the RNPS. Reaction (1) is used in remote monitoring of the operation of a reactor by methods that are being developed for the RNPS.[6,7] It is also used in searches for neutrino oscillations, the possible existence of which was hypothesized by Pontecorvo as far back as the late 1950s.[8] These oscillations are at present the center of attention from both the experimental and theoretical points of view as a manifestation of the mixing of massive neutral leptons. The range of problems related to these oscillations also includes the deficiency of solar neutrinos, the question of hidden mass and the inhomogeneous structure of the Universe, the nature of neutrinos (Dirac and Majorana neutrinos), the double (neutrino-free) beta decay of nuclei, and the magnetic moment of the neutrino.

Neutrino oscillations are impossible in the minimal standard model combining weak and electromagnetic interactions: the neutrino is massless and its leptonic charge is strictly conserved. The detection of neutrino oscillations would therefore signify the emergence of fundamentally new physics, outside the framework of the minimal model.

Numerous experimental searches for these oscillations have been carried out in recent years on high-energy charged-particle accelerators. On the other hand, the low energy of reactor neutrinos enables us to move into the region of low mass parameters that have not so far been accessible to accelerators.

2. The particular feature of experiments with reactor neutrinos $\tilde{\nu}_e$ is that the cross section for reaction (1), by which it is detected, is lower by a factor of 10^{19} than that for other neutral particles, and the energy of the reaction byproducts corresponds to the region of high natural radioactivity of materials and high intensity of neutrons and gamma rays due to cosmic muons. The consequence of this is that neutrino experiments performed on reactors belong to a small number of unique experiments. In 1982–1986, there were only two other groups (apart from the Rovno group) that had published the results of such experiments. These were the CALTECH-SIN-TUM collaboration (CST), working

 0038-5646/88/020213-09$04.00

on a reactor in Switzerland,[9] and a group carrying out experiments in France. In 1984, the French group reported that the intensity of the $\tilde{\nu}_e$ flux, measured at 13 and 18 m from the reactor, was not equal to the expected intensity deduced from geometric considerations, and ascribed this to neutrino oscillations.[10,11] The CST collaboration found no anomalies at other distances from the reactor.

3. Part of the preliminary results, obtained on RNPS were published earlier in Refs. 12–14. In the present paper, we report the results of a series of experiments completed toward the end of 1986. All the data were analyzed again using a unified approach. Two neutrino detectors were employed, namely, an integrating detector that recorded only the neutrons from reaction (1) and was used to measure the total cross section, and a scintillation-counter spectrometer that was used to obtain both the total and differential cross sections (Fig. 1). Both absolute and relative measurements were made of the intensity of the antineutrinos $\tilde{\nu}_e$ and of the positron spectra at two different distances from the reactor.

Five experiments were performed in 1984–1986. Two of them employed the integrating detector at a distance of 18 m from the center of the pile (experiments 1I and 2I). Measurements with the scintillation-counter spectrometer were carried out at 18 m (experiment 1S), 25 m (2S), and, at the end of the series, again at a distance of 18 m (3S). A total of 10^5 events corresponding to reaction (1) was recorded.

II. REACTION CROSS SECTION

The cross section (2) for monoenergetic $\tilde{\nu}_e$ can be normalized to the half-life t of the free neutron, using the well-known expression

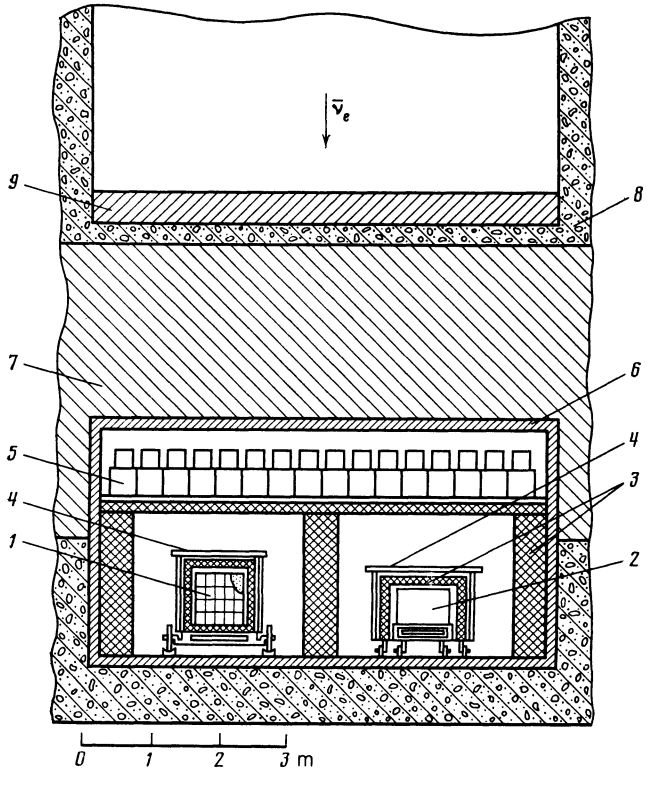

FIG. 1. Schematic diagram of the experimental setup: 1—integrating detector; 2—scintillation-counter spectrometer; 3—polyethylene; 4—scintillators of the anticoincidence shield; 5—tanks containing the liquid scintillator (anticoincidence "hood"); 6—steel; 7—heavy concrete; 8—concrete; 9—additional shielding.

$$ft=2\pi^3 \ln 2/m_e^5(g_V^2+3g_A^2).$$

According to Wilkinson,[15] $f=1.7146(\pm 10^{-2}\%)$ is a dimensionless phase volume factor. Assuming that $t^{\exp}=623$ s $(\pm 2\%)$, we find that, in absolute units, $(g_V^2+3g_A^2)^{1/2}=3.394\cdot 10^{-49}$ erg·m^3. Hence,

$$\sigma_0(E_\nu)=A\cdot 9.42(E_\nu-1.293)$$
$$\times[(E_\nu-1.293)^2-0.511^2]^{1/2}\cdot 10^{-44}\ \text{cm}^2, \quad (4)$$

where E_ν is in MeV and

$$A=623\ \text{c}/t=(g_V^2+3g_A^2)/(3.394\cdot 10^{-49})^2. \quad (5)$$

For energies $E_\nu \leqslant 10$ MeV, and to an uncertainty of about 0.1%, Fayans[16] took into account radiative corrections, recoils, and the contribution of weak magnetism to the reaction cross section (see also the work of Vogel[17]). The corrected cross section can be written in the form

$$\sigma(E_\nu)=\sigma_0(E_\nu)(1+\delta), \quad (6)$$

where δ varies smoothly from $\delta\simeq -0$–01 at $E_\nu=2$ MeV to $\delta\simeq -0.07$ at $E_\nu=10$ MeV. When this correction is introduced, g_V and g_A retain their meaning as the two constants corresponding to zero momentum transfer.

When recoils are taken into account, the relation between positron and neutrino energies becomes

$$\bar{E}_e=E_\nu-1.293-\bar{r}_n\ (\text{MeV}), \quad (7)$$

where $\bar{r}_n$ is the mean energy transferred to the neutron, which varies from about 7 keV at $E_\nu=3$ MeV to 90 keV at $E_\nu=10$ MeV. Although $\bar{r}_n \ll E_e$, the correction to the hard part of the positron spectrum can be up to 10% or more because the $\tilde{\nu}_e$ spectrum is very steep in this region and even a small energy shift is significant.

III. NUCLEAR REACTOR AS A SOURCE OF NEUTRINOS

1. The nuclear reactor is a pure source of electron antineutrinos: the neutron-rich fission fragments undergo β^- decays along their path toward beta-stability. (The percentage of $\tilde{\nu}_e$ electron neutrinos at energies above the threshold for reaction (1) is less than 0.01%.) Out of the approximately six electron antineutrinos per fission of the original nucleus, only three have energies above 1.8 MeV, i.e., above the threshold for reaction (1). Neutron capture in the pile materials produces practically no $\tilde{\nu}_e$ with energies above the threshold. The quasiequilibrium spectrum of the $\tilde{\nu}_e$ is established after a few hours of operation of the reactor at a given power level.

Apart from the contribution due to ^{235}U, the $\tilde{\nu}_e$ spectrum includes contributions due to three other fissile isotopes, namely, ^{239}Pu, ^{238}U, and ^{241}Pu. The ratio of these isotopes does not remain constant in time: as ^{235}U burns up, the contributions due to ^{239}Pu and ^{241}Pu are found to increase. The combined contribution of ^{235}U and ^{239}Pu is about 90%.

A typical reactor run is about twelve months, after which the reactor is shut down for a month for partial fuel replacement.

The energy spectra of the $\tilde{\nu}_e$ from fragments of different fissile nuclei differ appreciably from one another. For example, ^{238}U has three more surplus neutrons than ^{235}U, and its fragments lie further away from the beta-stability line. On

average, they emit more $\tilde{\nu}_e$ and with higher energies. In the case of ^{239}Pu, the $\tilde{\nu}_e$ spectrum is softer for similar reasons than that of ^{235}U. These features were first noted in the course of the RNPS experiments.[6,18]

2. The number of events corresponding to reaction (1) and recorded by the detector per unit time is related to the thermal power W of the reactor by

$$n_\nu = \frac{W}{\bar{E}_f}\frac{1}{4\pi\overline{R^2}}\bar{\sigma}_f N_H \varepsilon, \qquad (8)$$

where N_H and ε are the detector parameters (number of hydrogen atoms in the target and detection efficiency), which will be examined in Sec. V. The other parameters are discussed below.

a. The nominal power output of the VVER-440 reactor is $W = 1375$ MW and is measured to within about 2% (here and henceforth, and unless otherwise indicated, all quoted uncertainties correspond to a confidence level of 68%).

b. $\bar{E}_f$ is the mean energy absorbed in the reactor per fission. This includes both prompt and delayed energy release:

$$\bar{E}_f = \sum \alpha_i {}^iE_f,$$

where α_i (i = 5, 9, 8, 1) are the fractions of ^{235}U, ^{239}U, ^{238}U, and ^{241}Pu in the total number of fissions, found in the usual way,[7] and ${}^iE_f$ is the energy absorbed per fission. According to Ref. 19, ${}^5E_f = 201.8 \pm 0.5$ MeV, ${}^9E_f = 210.3 \pm 0.6$ MeV, ${}^8E_f = 205.3 \pm 0.7$ MeV, ${}^1E_f = 212.6 \pm 0.7$ MeV. Figures 2a and b show the variation in the contributions of α_i and $\bar{E}_f$ for a typical reactor run.

c. $1/4\pi\,\overline{R^2}$ is a geometric factor governing the flux intercepted by the detector; it is determined with allowance for the true energy release distribution in the reactor core. The difference from point geometry amounts to about 1% in our experiments. The distances $(\overline{R^2})^{1/2}$ are listed in Table V (see Sec. VI).

d. $\bar{\sigma}_f$ is the cross section per fission, measured in the experiment. It can be calculated if we know the isotopic composition of the nuclear fuel and the spectra ${}^i\rho_\nu(E_\nu)$ of the fragment mixture of the given fissile nucleus:

$$\bar{\sigma}_f = \sum \alpha_i {}^i\sigma_f = \sum \alpha_i \int {}^i\rho_\nu(E_\nu)\,\sigma(E_\nu)\,dE_\nu.$$

3. The spectrum ${}^i\rho_\nu$ at the "time of creation" of the $\tilde{\nu}_e$ can be found for a given fissile nucleus by summing the spectra of the individual fragments with allowance for the probability of their production on fission.[20–22] The lack of detailed information (mostly on the decay schemes of many of the short-lived isotopes) forces us to resort to assumptions whose validity is difficult to establish. The resulting uncertainty may reach 10–20% in the main part of the spectrum, which is unsatisfactory.

However, numerical simulation can be used to find a simple algorithm that relates the spectrum ρ_ν and the analogous resultant spectrum ρ_β of beta-electrons produced simultaneously during the decay of the fragments. It has been found that the ratio $K_{\nu\beta} = \rho_\nu(E)/\rho_\beta(E)$ is practically independent of the assumptions introduced about the unknown decay scheme.[21,23] It is clear from Fig. 3 that the values of this ratio found by independent calculation fall into a band of width $\pm$ 2–3% in the energy range up to 7 MeV, and this band includes both ^{235}U and ^{239}Pu. It is noticeable that $K_{\nu\beta}$ is not very energy-dependent even though the spectra themselves change by three orders of magnitude.

For the "true" neutrino spectra of ^{235}U and ^{239}Pu, we take the spectra reconstructed in the above way from the β-ray spectra ${}^5\rho_\beta$ and ${}^9\rho_\beta$ recorded at the Laue-Langevin Institute with a magnetic spectrometer.[24,25] The β-ray spectra of ^{238}U and ^{241}Pu were not measured and, for them, the true $\tilde{\nu}_e$ spectra were taken to be those calculated in Ref. 21, multiplied by the factor ${}^5\rho_\nu^{true}/{}^5\rho_\nu^{calc}$, where ${}^5\rho_\nu^{calc}$ is the calculated spectrum from Ref. 21, obtained in the same way as ${}^8\rho_\nu$ and ${}^1\rho_\nu$.

Table I lists the theoretical cross sections for fissile isotopes, obtained by combining the spectra ${}^i\rho_\nu$ with the cross section $\sigma(E_\nu)$ (6) for $A = 1$.

The uncertainties in the cross sections for the main isotopes ^{235}U and ^{239}Pu include the possibly somewhat underestimated uncertainties in the reconstructed $\tilde{\nu}_e$ spectra[24,25] and the uncertainty in the neutron half-life (2%). We note that, because of the fundamental importance of the problem, it would be desirable to have new measurements of the beta

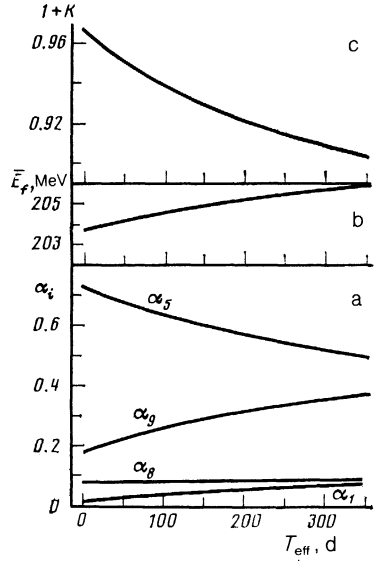

FIG. 2. Reactor parameters as functions of time during a reactor run: a—α_i—contributions of ^{235}U, ^{239}Pu, ^{238}U, and ^{241}Pu to the total number of fissions; b—mean energy $\bar{E}_f$ absorbed in the reactor per fission; c—1 + K, see (9) in text. The numbers next to the curves in Fig. 2a identify the particular isotope to which each curve refers.

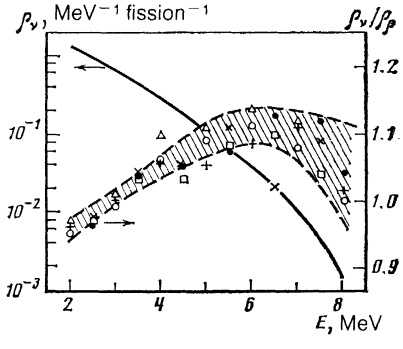

FIG. 3. Ratio of $\tilde{\nu}_e$ energy spectra to beta-particle spectra for an equilibrium mixture of fragments, and the $\tilde{\nu}_e$ spectrum as functions of the combined beta-particle and $\tilde{\nu}_e$ energies. ^{235}U: △—[20]; ○—[21]; +—[22]; ●—[24]; ^{239}Pu: ×—[21]; □—[22].

TABLE I. Cross section ${}^i\sigma_f^{\text{theor}}$ (in units of 10^{-43} cm^2 fission^{-1}) for the $\tilde{\nu}_e$ spectrum of fissile isotopes (calculated).

Isotope	^{235}U	^{239}Pu	^{238}U	^{241}Pu
${}^i\bar{\sigma}_f^{\text{theor}}$	6.31±3.4%	4.11±3.5%	8.83±10%	6.32±10%
${}^i\sigma_f^{\text{theor}}/{}^5\sigma_f^{\text{theor}}$	1.00	0.65±0.03	1.40±0.1	1.00±0.1

spectra of fragments and a more detailed analysis of the procedure for reconstructing the $\tilde{\nu}_e$ spectra.

We now reproduce once again the relationship between the cross section ${}^5\sigma_f$ of the main isotope and the average cross section $\bar{\sigma}_f$ evaluated over the isotope mixture:

$$\bar{\sigma}_f = \sum \alpha_i {}^i\sigma_f = {}^5\sigma_f \left[1 + \sum \alpha_i ({}^i\sigma_f/{}^5\sigma_f - 1)\right] \equiv {}^5\sigma_f(1+K). \tag{9}$$

Figure 2c shows the variation of $1 + K$ during the reactor run. It is clear that it can differ from the mean (over the run) by $\pm 3\%$.

IV. OSCILLATIONS

We shall consider the model[26] of two interfering states, ν_1 and ν_2, with masses m_1 and m_2:

$$\tilde{\nu}_e = \nu_1 \cos\theta + \nu_2 \sin\theta, \quad \tilde{\nu}_\mu = -\nu_1 \sin\theta + \nu_2 \cos\theta, \tag{10}$$

where θ is the mixing angle and $\tilde{\nu}_\mu$ is the muon antineutrino.

In free space, the intensity of the antineutrinos $\tilde{\nu}_e$ that are only just recorded by the detectors undergoes the periodic variation

$$I = I_0[1 - {}^1/_2 \sin^2 2\theta (1 - \cos 2\pi R/L)], \tag{11}$$

where I_0 is the intensity in the absence of the oscillations, R is the distance from the point of creation (point of observation), and L is the oscillation length. In more convenient units,

$$L = 2.5E_\nu/\Delta^2, \quad I = I_0[1 - \sin^2 2\theta \sin^2(1.27R\Delta^2/E_\nu)], \tag{12}$$

where $\Delta^2 = |m_1^2 - m_2^2|$ is measured in (eV)^2, L in meters, and E_ν in MeV. In the reactor experiment, the oscillations distort the positron spectrum as follows:

$$S_e = S_0\{1 - \sin^2 2\theta \sin^2[1.27R\Delta^2/(E_e + 1.29)]\}, \tag{13}$$

and reduce the intensity (cross section) as follows:

$$\sigma = \sigma_0[1 - f(R\Delta^2)\sin^2 2\theta], \tag{14}$$

where f represents the factor $\sin^2[1.27R\Delta^2/(E_e + 1.29)]$, averaged over the geometry and weighted over the spectrum of the positrons, which is almost independent of the form of the spectrum of the reactor $\tilde{\nu}_e$. For small $R\Delta^2$, we have $f \approx 0.1 \cdot (R\Delta^2)^2$, whereas, for $R\Delta^2 \gtrsim 20$ m·eV^2, the factor is $f \simeq 0.5$. For a given distance from the reactor, there is a range of values of Δ^2 in which the shape of the spectrum is sensitive to the oscillations. For large Δ^2, the oscillation effect is averaged out because of the finite resolving power of the spectrometer and the fact that we are not dealing with a point source. As a result, the spectrum as a whole is suppressed by the factor $1 - 1/2 \sin^2 2\theta$.

V. NEUTRINO DETECTION

1. Since the early reactor experiments, the neutrino detectors have become increasingly complicated and an increasing number of criteria has been introduced for selecting useful events (see, especially, the detector of Nezrick and Reines[3] and the CST spectrometer[9]). In contrast, the detectors used in the Rovno experiments are exceedingly simple and use a minimum number of relatively "soft" criteria for the selection of neutrino events. Discrimination against the background is largely transferred to external devices, i.e., passive and active shielding (anticoincidence system). This approach has substantially increased the detection efficiency, so that, with the relatively small target mass (190 kg), we are able to record the satisfactory count rate of 300×10^{-5}–500×10^{-5} s^{-1} in the relatively weak $\tilde{\nu}_e$ flux of 6×10^{12} cm^{-2} s^{-1} (at 18 m from the reactor). The other feature of the Rovno experiment is that we use two different detectors in the same $\tilde{\nu}_e$ flux. This improves the reliability and precision of the results in this difficult area.

2. In experiments 1I, 2I, 1S, and 3S, the detectors, i.e., the integrating detector ID and the scintillation-counter spectrometer SC are located in a chamber of $6.7 \times 6.7 \times 3.4$ m, separated from the reactor by a shield consisting of concrete containing steel fragments, the shielding thickness being 12 m of water equivalent (Fig. 1). Special experiments with a higher degree of shielding (9 in Fig. 1), and separate shielding of the detectors, showed that the effects due to neutrons and γ-rays from the reactor was less than 1% of the counting rate due to neutrino events. To reduce the radiation due to the natural radioactivity of concrete, the inner part of the chamber was faced with steel (160 mm). The immediate environment of the detectors consisted, as far as possible, of low-radiation light materials (polyethylene and plexiglas), which reduced the generation of neutrons by cosmic-ray muons. The anticoincidence system of each detector incorporated a "hood" of $3.2 \times 3.2 \times 0.5$ m^3 and six plates of the methyl methacryllate phosphor. When a muon or a shower passes through, the anticoincidence circuit cuts off the detectors for 200 μs (ID) on 6 μs (SC). The number of such events (300–500 s^{-1}) is independent of the reactor output.

3. The target for the $\tilde{\nu}_e$ and the moderator for neutrons from reaction (1) in the integrating detector is made from polyethylene and contains proportional counters (32 mm in diameter, sensitive length 1000 mm), filled with ^{3}He and argon at partial pressures of 4 and 0.7 atm, respectively (Fig. 4a). The neutrons are recorded by the counters, using the byproducts of the reaction $n + {}^3\text{He} \rightarrow p + T + 0.765$ MeV. The counters in the polyethylene target form a rectangular array with a period of 45 mm.

The product of the number of hydrogen atoms and the

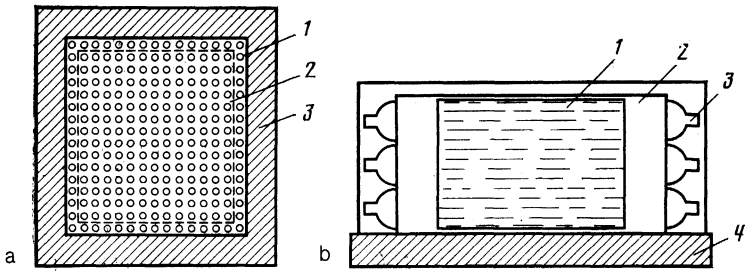

FIG. 4. Schematic diagram of the detectors: a—integrating detector; 1—proportional counter filled with ^{3}He; 2—polyethylene; 3—borated polyethylene; b—scintillation-counter spectrometer: 1—liquid scintillator; 2—lightguide; 3—FEU-49B; 4—borated polyethylene.

detector efficiency, $N_H\varepsilon$, is the main parameter of the detector in absolute cross-section measurements [see (8)]. The detection efficiency ε is difficult to determine accurately by calculation, partly because of uncertainties at the detector faces where neutrons are lost. We therefore define the central portion of the detector (indicated by the broken lines in Fig. 4a) and only the counts produced by this part are used in the determination of the cross section. Uncompensated escapes from the region, $\xi = (3 \pm 1)\cdot 10^{-2}$, occur only through the two end faces, 1000 m apart. The total efficiency of detection of neutrons from reaction (1) can be conveniently written in the form $\varepsilon = \varepsilon_\infty (1 - \xi)\gamma$, where ε_∞ is the detector efficiency without surface losses (infinite detector) and γ is the amplitude sampling coefficient. The experimental results are: $\varepsilon_\infty = 0.808 \pm 0.12$, $\gamma = 0.690 \pm 0.01$ (1S), and $\gamma = 0.725 \pm 0.01$ (2I). Further details can be found in Ref. 14. The total detection efficiency was just over 50% (Table II). The uncertainty in the number of protons is due to counter end errors and amounts to $\pm 2\%$. Thus, the product $N_H\varepsilon$ was determined to within 3.1%.

In addition to the amplitude selection of events in the detector, we also examined the multiplicity of these events. We used only single events not accompanied by further pulses for 200 μs. The magnitude of the neutrino effect was determined as the difference between the counting rate with the reactor respectively running and shut down (Fig. 5). Discrimination against the detection of positrons is very attractive from the point of view of determining the total cross section for reaction (1) because this obviates difficulties connected with the positron detection threshold. On the other hand, it reduces the effect-to-background ratio and imposes more stringent conditions on stability during long-term measurements.

4. The scintillation-counter spectrometer used in these measurements was a modernized version of the detector first built by Reines and Cohen in 1953. The liquid organic scintillator (LOS) performs the functions of a target, positron spectrometer, moderator, and neutron detector. Neutrons were recorded by counting γ-rays (total energy $E \simeq 8$ MeV) due to capture by gadolinium nuclei in the LOS. The LOS consists mostly of paraffin oil with a density of 0.8 g/cm^3 and has a hydrogen-to-carbon ratio of 1.9. The body of the detector is made from transparent plexiglas. The LOS volume is 238 liters (700 × 500 × 680 mm). The two opposite windows on which twelve FEU-49B photomultipliers were placed have a thickness of 150 mm each. This equalizes light collection and partially protects the LOS from the natural radioactivity of the photomultipliers (Fig. 4b).

Events such as (1) are recorded by delayed positron-neutron coincidences. The mean lifetime of the neutron before capture is 50 μs. Any event with an amplitude corresponding to an energy release of 0.9–10 MeV triggers the detection cycle. The frequency of such trigger events is 24 s^{-1}. After a short delay, the trigger event opens, for 1000 μs, the normally closed system for detecting the second event, which is recorded in the range 2.7–10 MeV. An event is classified as "effect + background" if the second event falls into the time interval between 0 and 200 μs ($\simeq 4\tau$) and as a "random background" if the second event falls into the interval 400–1000 μs (8τ–20τ). The detector count rate above the detection threshold for the second event is about 0.8 s^{-1}. A

TABLE II. Parameters of experiments 1I–3S.

Experiment	1I	2I	1S	2S	3S
Target	CH_2	CH_2	LOS	LOS	LOS
N_H (10^{28})	1.152	1.591	1.570	1.570	1.560
ε	0.540	0.568	0.321	0.321	0.322
$(\bar{R}^2)^{1/2}$, m	18.0	17.96	18.15	25.17	18.18
$\bar{W}$, MW	1379	1371	1371	1378	1452
Number of recorded $\tilde{\nu}_e$, thousands	13.7	12.8	15.2	16.4	20.4
Counting rate n_ν (in 10^5 s)	361.4	561.5	303.5	165.6	309.5

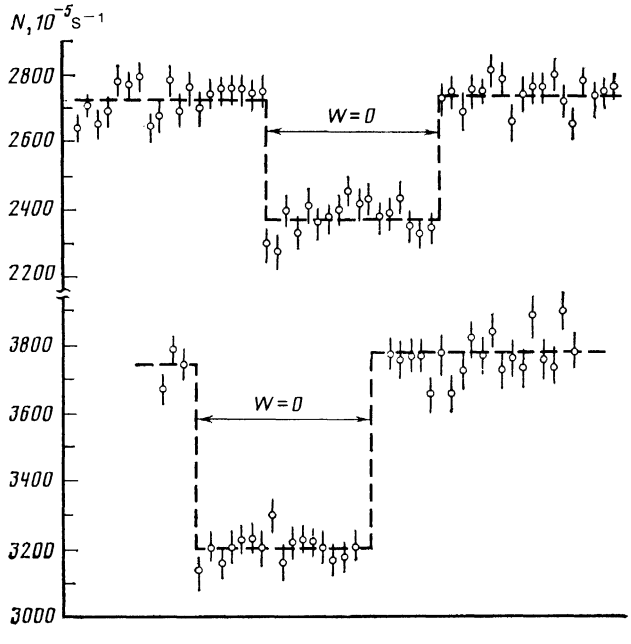

FIG. 5. Counting rate recorded by the integrating detector (in 10^5 s) with the reactor running and shut down, respectively, in experiments 1I (upper curve) and 2I.

minicomputer stores the amplitudes of the first and second events and the time between them.

5. The absolute energy scale of the spectrometer was calibrated, after correction for the spatial inhomogeneity of light collection, using a thin ^{144}Ce beta-ray source (endpoint energy 3.00 MeV) which could be placed at different points within the working volume. The uncertainty in the absolute scale was 1.4% and its stability was monitored against ^{60}Co γ-rays (1.17 MeV and 1.33 MeV), ^{24}Na γ-rays (1.38 MeV and 2.75 MeV), and the γ-ray spectrum due to neutron capture in Gd. The energy scales in experiments 2S and 3S agree with one another to within 0.7%. The scale in experiment 1S was found to differ by 3% and was corrected during the analysis.

6. The efficiency $\varepsilon_{\nu p}$ with which events such as (1) were recorded and the response function r of the spectrometer were found by numerical simulation of the fate of the neutron and positron, normalized against special experiments with sources of neutrons (^{252}Cf) and γ- rays. We now reproduce the results together with some comments but without going into details of the calculations and control experiments.

The detection efficiency depends on the energy thresholds E_e^{th} and E_n^{th} for the detection of positrons and neutrons, respectively, and on the neutron detection time t: $\varepsilon_{\nu p} = (E_e^{\text{th}}, E_n^{\text{th}}, t)$. It is convenient to write it in the form

$$\varepsilon = (1-\alpha_t)\,(1-\alpha_\beta)\,\varepsilon\,(0, E_n^{\text{th}}).$$

The first factor involves $\alpha_t = 0.054 \pm 20\%$ and represents events outside the time interval in which the second events are recorded. The second factor contains $\alpha_\beta = 0.105 \pm 20\%$ and represents events in which the positrons have kinetic energies less than 0.6 MeV and are under the detection threshold; $\varepsilon(0, E_n^{\text{th}}) = 0.379 \pm 5\%$. The final result is $\varepsilon = 0.946 \cdot 0.895 \cdot 0.379 = 0.321 \pm 5.5\%$.

The response function $r(T, E)$, where E is the observed energy, is a measure of the reaction of the spectrometer to monoenergetic positrons with kinetic energy T. The center of gravity of the function r is shifted relative to T by 0.5 MeV toward higher energies. The response function has little effect on the shape of the positron spectrum (in the absence of oscillations). For large Δ^2, it averages out the modulation of the spectrum and makes its shape insensitive to Δ^2.

In the calculation, the values of ε and r are found by averaging the products $\varepsilon_\beta(x)\varepsilon_n(x)$ and $r_\beta(x)\varepsilon_n(x)$, where x is the point at which the reaction takes place. In the calculation of the efficiency and response function, allowance is made for the partial loss of annihilation photons, the inhomogeneous light collection, the intrinsic energy resolution of the spectrometer, and partial loss of energy by the positron in the material of the body (wall effect). Soft bremsstrahlung photons and positron annihilation in flight are neglected. The latter effect increases linearly with positron energy and, on average, amounts to 2.5%. It is partially compensated by the absorption of γ-rays in the working volume.

The concentration n_{H} of hydrogen atoms (cm^{-3}) in the scintillator determines the total number N_{H} of hydrogen atoms in the target and the properties of the LOS as a neutron moderator. It was found to within 1.5% by a physical method, directly in the working volume.[2)] This was done by measuring the time distribution of neutron-capture events in hydrogen ($n + p \to d + 2.23$ MeV): $\varphi_{\text{H}}(t) \sim \exp(-\lambda_{\text{H}} t)$, where $\lambda_{\text{H}} = \sigma_{\text{H}}(v) v n_{\text{H}} = \text{const}$, since $\sigma_{\text{H}}(v) \sim 1/v$, and the product $\sigma_{\text{H}} v$ is known[27] to better than 0.5% (v is the neutron velocity).

Direct calculation of the absorption of thermal and epithermal neutrons in the LOS containing Gd is difficult because neutron thermalization is not known in detail and the capture cross section $\sigma_{n\gamma}(v)$ of Gd is a rapidly-varying function of neutron velocity in this region. The grouping $\lambda_{\text{Gd}} = n_{\text{Gd}} \sigma_{n\gamma}(v) v$ appears directly in the measured neutron-capture time distribution function $\varphi_{\text{Gd}}(t)$ (Fig. 6), where n_{Gd} is the concentration of the Gd atoms. It can be shown that the fraction of captures in Gd relative to the total number of captures in the LOS is

$$\eta_{\text{Gd}} = \left[\int \varphi_{\text{Gd}}(t)\, e^{\lambda_{\text{H}} t} dt\right]^{-1},$$

where λ_{H} is the measured probability of capture in hydrogen and $\int \varphi_{\text{Gd}} dt = 1$.

VI. RESULTS

1. Data typical of the individual experiments are listed in Table II. The results selected for analysis were those obtained when the reactor was working at near-nominal power. Small corrections representing the contribution of the other reactor on the RNPS area were introduced into the measured count rate n_ν, and (8) was used to calculate the cross section $\bar{\sigma}_f^{\text{exp}}$. The values obtained in this way are listed in Table III. The first uncertainty in $\bar{\sigma}_f$ (2.2%) is the same in all the experiments and represents the uncertainty in the measured reactor power and the geometric uncertainty. The second is due to errors in the detector characteristics and fluctuations.

The cross section averaged over the 1I, 2I, 1S, and 3S experiments is

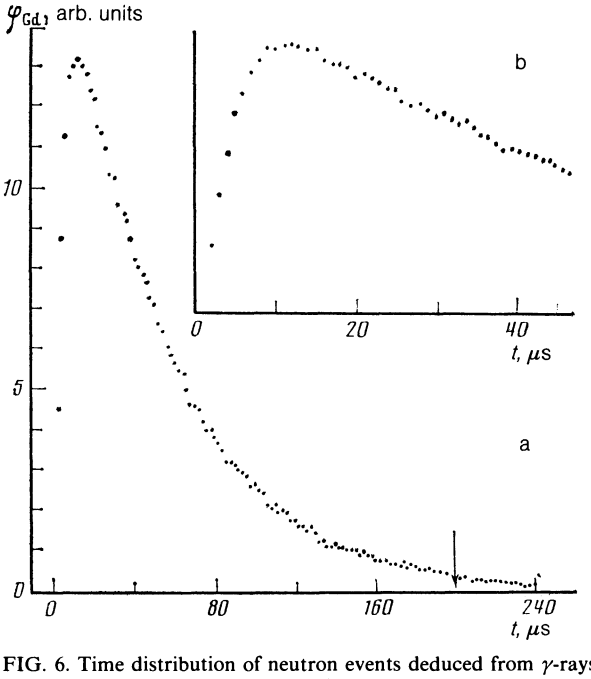

FIG. 6. Time distribution of neutron events deduced from γ-rays from captures in gadolinium. The thermalization effect can be seen. The arrow shows the limit of the time interval for "effect + background" (see text).

TABLE III. Fraction of fissile isotopes, α_i, the energy per fission $\bar{E}_f$ (MeV), and values of $\bar{\sigma}_f^{exp}$ (10^{-43} cm^2 fission^{-1}).

Experiment	α_5	α_9	α_8	α_1	$\bar{E}_f$	$\bar{\sigma}_f^{exp}$
1I	0.607	0.277	0.074	0.042	204.8	5.70±2.2%±6%
2I	0.603	0.276	0.076	0.045	204.9	5.89±2.2%±6%
1S	0.606	0.277	0.074	0.043	204.8	6.04±2.2%±7%
2S	0.557	0.313	0.076	0.054	205.2	5.96±2.2%±7%
3S	0.606	0.274	0.074	0.046	204.9	5.83±2.2%±6.4%

$$\bar{\sigma}_f = (5.86 \pm 2.2\% \pm 4\%) \cdot 10^{-43} \text{ cm}^2 \text{ fission}^{-1}.$$

Combining the squares of the errors, we finally obtain

$$\bar{\sigma}_f^{exp} = (5.86 \pm 4.6\%) \cdot 10^{-43} \text{ cm}^2 \text{ fission}^{-1} \quad (R = 18 \text{ m}). \tag{15}$$

This cross section refers to the nuclear fuel of the following composition:

$$\alpha_5 = 0.606,\ \alpha_9 = 0.276,\ \alpha_8 = 0.075,\ \alpha_1 = 0.043. \tag{16}$$

Following tradition, we give the cross section converted to the spectrum of ^{235}U:

$$^5\sigma_f = 6.28 \pm 5\% \cdot 10^{-43} \text{ cm}^2 \text{ fission}^{-1}.$$

The theoretical (expected) cross section for the mixture (16) is

$$\bar{\sigma}_f^{theor} = (5.89 \pm 3.7\%) \cdot 10^{-43} \text{ cm}^2 \text{ fission}^{-1}, \tag{17}$$

where the uncertainty includes both errors in the spectra and in the neutron half-life: $t = 623 \text{ s} \pm 2\%$. The ratio of intensities at 25 and 18 m from the reactor, corrected for the geometry and for the small difference in the composition of the nuclear fuel (Table III) was found to be $^{25}I/^{18}I = 1.013 \pm 4\%$.

The energy spectra were measured in experiments 1S, 2S, and 3S with the reactor running (effect + background) and with the reactor shut down (background). As an example, Fig. 7 shows the spectra obtained in experiment 3S. The spectra of positrons from reaction (1) were obtained by subtracting the background. Comparison of the positron spectra recorded in experiments 1S and 3S at 18 m from the reactor after an interval of two years showed that they were identical to within the experimental uncertainty. We therefore took an average of these experimental results (Fig. 8). It is clear from these data that the calculated spectra are in satisfactory agreement with experiment in the energy interval $E_e = 1.2$–6 MeV ($E_\nu = 2.5$–7.3 MeV). At higher energies, both experimental and theoretical uncertainties increase rapidly, and the question of agreement remains open.

2. Before we turn to the analysis of the situation in relation to neutrino oscillations, we must draw certain conclusions. It follows from (15) and (17) that

$$\bar{\sigma}_f^{exp}/\bar{\sigma}_f^{theor} = 0.995 \pm 0.060, \tag{18}$$

i.e., the probabilities of neutron decay and the inverse reaction (1) are equal to within 6%. From (18) and (5), we find that

$$\mathring{A} = \frac{(g_V^2 + 3g_A^2)}{(3.394 \cdot 10^{-49})^2} = 0.995 \pm 0\,058.$$

Since $g_V = 1.4127 \pm 0.0003) \cdot 10^{-49}$ erg·cm^3,

$$g_A^{vp} = 1.775 \cdot 10^{-49} \text{ erg/cm}^3, \pm 3.5\%,$$

where the index vp indicates that the constant was deduced from inverse beta-decay. The corresponding half-life was found to be 626 s ± 5.8%.

3. We now turn to the question of oscillations. We use two methods of analysis: absolute and relative. In the first, the results of absolute measurements are compared with their expected values. The results of the analysis depend on the $\tilde{\nu}_e$ spectra, the detection efficiency, and so on. When the relative method is employed, we compare the spectra (and intensities) measured at 18 and 25 m from the reactor. The results are then more reliable but provide information on the oscillation parameters in a narrower range of their values.

a. Absolute method. Let us first reproduce the results obtained by comparing the total cross sections. It follows from (18) and (14) that $f(R\Delta^2)\sin^2 2\theta \leqslant 0.065$ (68% confidence level). The limits on the oscillation parameters, de-

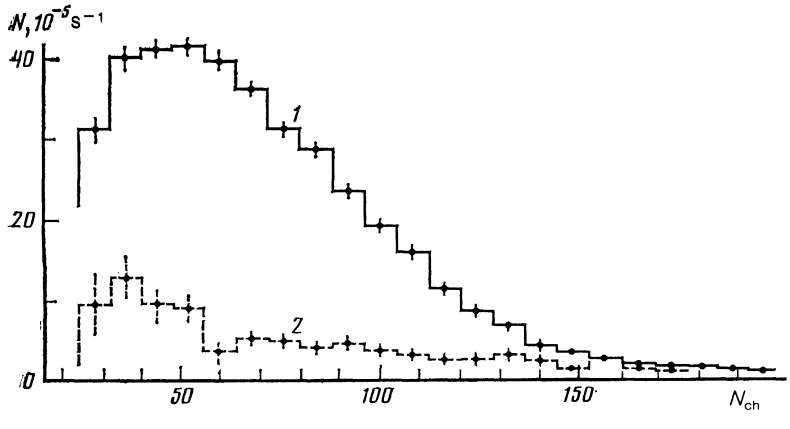

FIG. 7. Spectra recorded in the 3S experiment: 1—reactor running ("effect + background"); 2—reactor shut down (background). The random coincidence background has been subtracted.

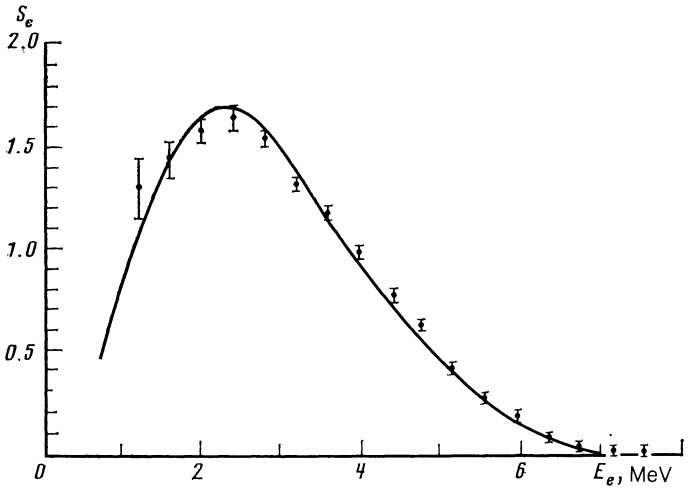

FIG. 8. Spectrum of positrons from reaction (1) at a distance of 18 m (in units of 10^{-43} cm^2 MeV^{-1} fission^{-1}). The points are averages over experiments 1S and 3S (points with error bars). Solid curve—calculated (expected) spectrum without taking oscillations into account.

duced from this inequality at the 90% confidence level, are shown in Fig. 9 (curve 3).

Next, we compare the positron spectrum S_{18}^{exp} at 18 m with the expected spectrum $S^{\text{theor}}(\theta, \Delta^2)$ (Fig. 10a). The method of maximum likelihood was employed to determine whether the oscillation parameters were normally distributed. The likelihood function was taken to be the usual χ^2 expression for the first 13 points of the positron spectrum in the energy interval 1–6 MeV in which we took into account variations in absolute normalization and in the energy scale to within experimental uncertainties and uncertainties in the $\tilde{\nu}_e$ spectrum. The resulting limits at the 90% confidence level are also shown in Fig. 9 (curve 2).

b. Relative method. The ratio $S_{25}^{\text{exp}}/S_{18}^{\text{exp}}$ of spectra measured at the two distances (Fig. 10b) was compared with the calculated ratio $S_{25}^{\text{theor}}(\theta, \Delta^2)/S_{18}^{\text{theor}}(\theta, \Delta^2)$. Here again, we used the maximum likelihood methods (χ^2 for 13 points) with allowance for variations in the relative normalization and the stability of the energy scale of the spectrometer. The results are shown in Fig. 9 (curve 1).

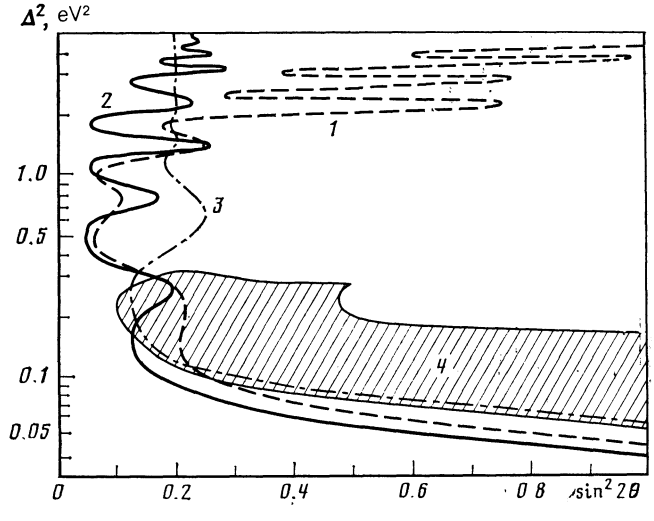

FIG. 9. Limits on the oscillation parameters Δ^2, $\sin^2\theta$ at the 90% confidence level. Regions to the right of the curves are forbidden. Curves obtained from: 1—ratio of spectra at 25 and 18 m (relative method); 2—comparison of S_{18}^{exp} with S_{18}^{theor} (absolute method); 3—comparison of measured and calculated cross sections at 18 m (absolute method). The shaded region (4) corresponds to the oscillation effect according to Ref. 10.

VII. CONCLUSION

The cross section for the reaction (1), calculated from the beta-decay half-life of the free neutron on the assumption of the V–A interaction with maximum parity violation, is in good agreement with our experimental value [see (18)]. The agreement between the probabilities of these mutually inverse processes is not trivial: other theoretical schemes examined recently [admixture of the $V+A$ interaction[28] and the $SU(2)_L \times SU(2)_R \times U(1)$ model] violate this relation.

Our limits on the oscillation parameters (see Fig. 9) do not confirm the reported[10] observation of oscillations in experiments at 13.6 and 18.3 m from a reactor. The results of the CTS collaboration,[9] which has carried out measurements at three distances in the range 37.9–64.7 m, also do not confirm the report given in Ref. 10. Nevertheless, we must exercise caution in our final conclusions because the experiments were performed at different distances and the comparison was made not between observed quantities, but

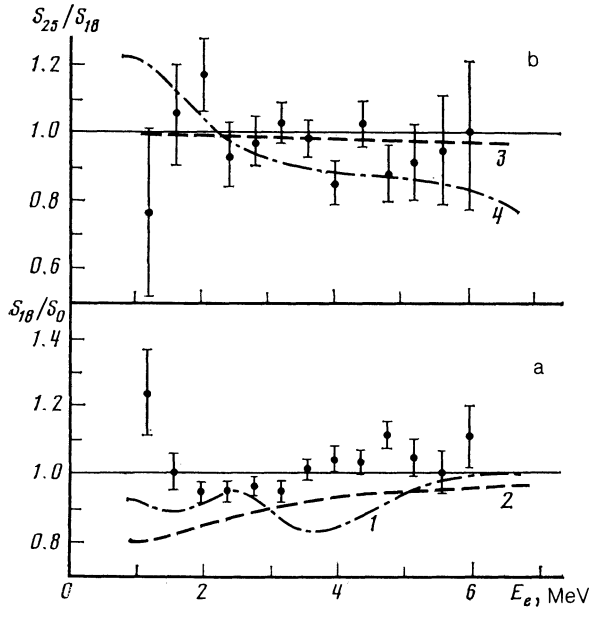

FIG. 10. Ratio of positron spectra (S_0 is the spectrum in the absence of oscillations). Points—experimental, curves—expected ratio of spectra for: 1—$\Delta^2 = 1$ eV^2, $\sin^2 2\theta = 0.2$; 2—$\Delta^2 = 0.15$ eV^2, $\sin^2 2\theta = 0.2$; 3—$\sin^2 2\theta = 0$ (no oscillations); 4—$\Delta^2 = 0.2$ eV^2, $\sin^2 2\theta = 0.25$.

between the results of an analysis with two oscillating states.

If the considerable deficiency in solar neutrinos reported by Davis[29] is due to oscillations,[30,26,8] but the parameters of the oscillations do not fall into the range in which the Mikheev-Smirnov amplification mechanism operates,[31] then $\sin^2 2\theta \sim 1$. The sensitivity in Δ^2 thus far obtained could be substantially improved by peforming experiments at distances of 1–2 km from the reactor. The number of events due to reaction (1) per ton of organic scintillator would then be 1–4 per day, i.e., greater by almost three orders of magnitude than that in the planned experiments on the detection of solar ("boron") neutrinos, using electrons from ν-e scattering.

If the deficiency of ν_e from the Sun is due to the Mikheev-Smirnov mechanism, which amplifies the $\nu_e \to \nu_\mu$ transitions in the range $\Delta^2 = (5\times 10^{-5}$–$10^{-7})$ eV^2, then the oscillation length $L_{\nu\mu} \gtrsim 200$ km is too large for a reactor experiment. However, the $\nu_e \to \nu_\tau$ transitions may then fall into the sensitivity band: Bethe's estimate,[32] based on the work of Gell-Mann *et al.*,[33] gives a much greater mass for the third-generation neutrino ν_3 than for ν_1 and ν_2. In order to detect the $\nu_e \to \nu_\tau$ vacuum oscillations, we must substantially increase the sensitivity to the mixing angle. It may be considered that this will be achieved in future experiments at distances not too great, and with improved statistics of recorded events and better energy resolution of the spectrometer.

The authors are greatly indebted to M. A. Markov for effective help at all stages of preparation and execution of the RNPS experiments. We are grateful to S. T. Belyaev for useful discussions, attention, and support, and to the Director and Staff of the RNPS for their constant help. The authors thank the Director and Staff of the Institute of Chemistry (at Ufa) for their help in connection with the scintillation counter technique, and O. A. Gunder and S. A. Malinovskaya for developing the solid phosphors. They are grateful to S. A. Rayans for discussions of theoretical aspects and to V. F. Apalin, A. A. Borov, and all the colleagues at the Science Division who have contributed to this research.

[1)]See Sec. II for a more precise statement of (2) and (3).

[2)]The scintillator was changed several times during the experiment. At first, the body of the detector was filled with a Gd-free LOS and then a concentrated solution of a complex salt of gadolinium with a total volume of about 2 liters was added.

[1]F. Reines and C. L. Cowan, Phys. Rev. **92**, 830 (1953).
[2]F. Reines and C. L. Cowan, Phys. Rev. **113**, 273 (1959).
[3]F. A. Nezrick and F. Reines, Phys. Rev. **142**, 852 (1966).
[4]A. I. Afonin, S. A. Bogatov, A. A. Borovoi *et al.*, Pis'ma Zh. Eksp. Teor. Fiz. **37**, 122 (1983) [JETP Lett. **37**, 150 (1983)].
[5]D. H. Wilkinson, M. Gell-Mann, and D. E. Alburger, Phys. Rev. C **18**, 401 (1978).
[6]L. A. Mikaelyan, Proc. Intern. Conf. Neutrino-77, Nauka, Moscow, 1978, Vol. 2, p. 383.
[7]V. A. Korovkin, S. A. Kodanev, A. D. Yarichin *et al.*, Atom. Energ. **56**, 214 (1984).
[8]B. M. Pontecorvo, Zh. Eksp. Teor. Fiz. **34**, 247 (1958) [JETP **7**, 172 (1958)].
[9]G. Zavek, F. Feilitzsch, R.L. Mössbauer *et al.*, Phys. Rev. D **34**, 2621 (1986).
[10]J. F. Cavaignac, A. Houmada, D. H. Koang *et al.*, Phys. Lett. B **148**, 387 (1984).
[11]D. H. Koang, *Weak and Electromagnetic Interaction in Nuclei*, ed. by H. V. Klapdor, Springer-Verlag, Heidelberg, 1986, p. 755.
[12]A. I. Afonin, A. A. Borovoi, Yu. L. Dobrynin *et al.*, Pis'ma Zh. Eksp. Teor. Fiz. **41**, 355 (1985) [JETP Lett. **41**, 435 (1985)].
[13]A. I. Afonin, S. A. Bogatov, A. A. Borovoi *et al.*, Yad. Fiz. **42**, 1138 (1985) [Sov. J. Nucl. Phys. **42**, 719 (1985)].
[14]S. M. Belen'kii, Yu. L. Dobrynin, L. A. Mikaelyan *et al.*, Yad. Fiz. **42**, 894 (1985) [Sov. J. Nucl.Phys. **42**, 567 (1985)].
[15]D. H. Wilkinson, Nucl. Phys. A **377**, 474 (1982).
[16]S. A. Fayans, Yad. Fiz. **42**, 929 (1985) [Sov. J. Nucl. Phys. **42**, 590 (1985)].
[17]P. Vogel, Phys. Rev. D **29**, 1918 (1984).
[18]A. A. Borovoĭ, Yu. L. Dobrynin, and V. I. Kopeĭkin, Yad. Fiz. **25**, 264 (1977) [Sov. J. Nucl. Phys. **25**, 144 (1977)].
[19]V. I . Kopeĭkin, Preprint IAE-4305/2 [in Russian], 1986.
[20]V. I. Kopeĭkin, Yad. Fiz. **32**, 1507 (1980) [Sov. J. Nucl. Phys. **32**, 780 (1980)].
[21]P. Vogel, G. K. Schenter, F. M. Mann, and R. E. Schenter, Phys. Rev. C **24**, 1543 (1981).
[22]H. V. Klapdor and J. Metzinger, Phys. Lett. B **112**, 22 (1982).
[23]A. A. Borovoĭ, V. I. Kopeĭkin, L. A. Mikaelyan, and S. V. Tolokonnikov, Yad. Fiz. **36**, 400 (1982) [Sov. J. Nucl. Phys. **36**, 232 (1982)].
[24]K. Schreckenbach, G. Colvin, W. Gelletly, and F. Feilitzsch, Phys. Lett. B **160**, 325 (1985).
[25]F. V. Feilitzsch, A. A. Hahn, and K. Schreckenbach, Phys. Lett. B **118**, 162 (1982).
[26]S. M. Bilen'kiĭ and B. M. Pontecorvo, Usp. Fiz. Nauk **123**, 181 (1977) [Sov. Phys. Usp. **20**, 776 (1977)].
[27]D. Cocinos and E. Melkonian, Phys. Rev. C **15**, 1636 (1977).
[28]A. A. Borovoĭ, Yu. L. Dobrynin, and V. I. Kopeĭkin, Yad. Fiz. **25**, 264 (1977) [Sov. J. Nucl. Phys. **25**, 144 (1977)].
[29]J. N. Bahcall, B. T. Cleveland, R. Davis, and J. K. Rowley, Astrophys. J. **292**, 179 (1985).
[30]S. M. Vilen'kiĭ and B. M. Pontecorvo, Yad. Fiz. **43**, 1225 (1986) [Sov. J. Nucl. Phys. **43**, 786 (1986)].
[31]S. P. Mikheev and Yu. A. Smirnov, Yad. Fiz. **42**, 1441 (1985) [Sov. J. Nucl. Phys. **42**, 913 (1985)].
[32]H. Bethe, Phys. Rev. Lett. **56**, 1305 (1986).
[33]M. Gell-Mann, P. Ramoud, and R. Slansky, in: *Supergravity*, ed. by P. van Nierwenhuizen and D. Z. Freedman, North-Holland, Amsterdam, 1979.

Translated by S. Chomet